Title

Fast detection of covert visuospatial attention using hybrid N2pc and SSVEP features

Journal

Journal of Neural Engineering, 13(6)

ISSN

1741-2560

Authors

Xu, Minpeng

Wang, Yijun

Nakanishi, Masaki

et al.

Publication Date

2016-12-01

DOI

10.1088/1741-2560/13/6/066003

Peer reviewed

Fast detection of covert visuospatial attention using hybrid N2pc and SSVEP features

2016 J. Neural Eng. 13 066003

(http://iopscience.iop.org/1741-2552/13/6/066003)

IOP Publishing Journal of Neural Engineering
J. Neural Eng. 13 (2016) 066003 (13pp) doi:10.1088/1741-2560/13/6/066003

Fast detection of covert visuospatial attention using hybrid N2pc and SSVEP features

Minpeng Xu[1,2], Yijun Wang[2,3,4], Masaki Nakanishi[2], Yu-Te Wang[2], Hongzhi Qi[1], Tzyy-Ping Jung[2] and Dong Ming[1,4]

[1] Department of Biomedical Engineering, Tianjin University, Tianjin 300072, People's Republic of China
[2] Swartz Center for Computational Neuroscience, University of California, San Diego, CA 92093, USA
[3] State Key Laboratory on Integrated Optoelectronics, Institute of Semiconductors, Chinese Academy of Sciences, Beijing 100083, People's Republic of China

E-mail: wangyj@semi.ac.cn and richardming@tju.edu.cn

Received 29 January 2016, revised 21 July 2016
Accepted for publication 5 September 2016
Published 5 October 2016

Abstract

Objective. Detecting the shift of covert visuospatial attention (CVSA) is vital for gaze-independent brain–computer interfaces (BCIs), which might be the only communication approach for severely disabled patients who cannot move their eyes. Although previous studies had demonstrated that it is feasible to use CVSA-related electroencephalography (EEG) features to control a BCI system, the communication speed remains very low. This study aims to improve the speed and accuracy of CVSA detection by fusing EEG features of N2pc and steady-state visual evoked potential (SSVEP). *Approach.* A new paradigm was designed to code the left and right CVSA with the N2pc and SSVEP features, which were then decoded by a classification strategy based on canonical correlation analysis. Eleven subjects were recruited to perform an offline experiment in this study. Temporal waves, amplitudes, and topographies for brain responses related to N2pc and SSVEP were analyzed. The classification accuracy derived from the hybrid EEG features (SSVEP and N2pc) was compared with those using the single EEG features (SSVEP or N2pc). *Main results.* The N2pc could be significantly enhanced under certain conditions of SSVEP modulations. The hybrid EEG features achieved significantly higher accuracy than the single features. It obtained an average accuracy of 72.9% by using a data length of 400 ms after the attention shift. Moreover, the average accuracy reached ~80% (peak values above 90%) when using 2 s long data. *Significance.* The results indicate that the combination of N2pc and SSVEP is effective for fast detection of CVSA. The proposed method could be a promising approach for implementing a gaze-independent BCI.

Keywords: brain–computer interface, covert visuospatial attention, gaze-independent, hybrid, N2pc, steady-state visual evoked potential (SSVEP)

(Some figures may appear in colour only in the online journal)

1. Introduction

Brain–computer interfaces (BCIs) can provide an alternative approach for patients who are severely disabled but preserve intact cognition [1, 2]. Currently, electroencephalography (EEG) is a preferable approach for BCIs than other non-invasive functional brain monitoring methods, because of its low requirements and acceptable properties of the recording system. BCIs based on event-related potentials (ERPs) [3], steady-state visual evoked potentials (SSVEPs) [4], and sensory motor rhythms [5] are the three most popular BCI paradigms.

In traditional views, reactive visual BCIs such as the P300-based BCI and the SSVEP-based BCI for healthy

[4] Author to whom any correspondence should be addressed.

people, could also be used by severely disabled patients as long as they are conscious. However, many studies have demonstrated that the traditional reactive BCIs are less effective for users who are unable to shift their overt attention from the central visual field, like the terminal amyotrophic lateral sclerosis (ALS) patient [6–8]. The main reason for the degraded performance is that, for patients who can only use the covert visual attention to observe the target character, brain responses to outside visual stimuli are much weaker than those who can use the overt visual attention. Specifically, the visual N1, which plays a vital role in the classification of the target versus non-target responses for the P300 speller, would be greatly compromised in the covert visual attention [8]. Similarly, the differences between the target and non-target SSVEPs would also be reduced during the covert visual attention, leading to significantly decreased performance. Therefore, most existing visual BCI systems work only for healthy people who have the ability to control their eye movements.

To overcome the aforementioned problems, efforts have been made to develop gaze-independent BCIs, which could be more effective for severely disabled patients. For instance, Kelly *et al* proposed to use the covert visuospatial attention (CVSA) modulated SSVEPs to perform a binary classification of the left versus right attention sides [9]. Later, Allison *et al* demonstrated that selective attention to one of two overlapping stimuli could also elicit sufficient SSVEP differences for BCI control [10]. Zhang *et al* developed an online gaze-independent BCI system based on SSVEPs modulated by selective visual attention in 2010 [11]. In 2014, the SSVEP-based gaze-independent BCI had a clinical test with locked-in patients [12]. However, only 1 out of 4 patients could perform online communication. For the field of transient ERP-based BCIs, most attention was paid to design new paradigms beyond the matrix speller, such as the Hex-o-Spell speller [13, 14], Cake Speller [15, 16], Center Speller [15], Geospel [17] and the rapid serial visual presentation [18], in which ERP classifications were completely dependent on the endogenous component like the P300 potential. In 2013, a clinical test of 10 ALS patients was conducted for the ERP-based gaze-independent BCI [19]. The results showed an average information transfer rate (ITR) of 6.3 bits min^{-1} after 4 d of training. The posterior alpha rhythm-based BCI is another important gaze-independent and stimulus-free system [20–23]. It is based on the fact that when people attend to one side, the contralateral alpha rhythm on the occipital area would decrease while the ipsilateral alpha rhythm would increase. So the hemispheric distribution of the posterior alpha power could be used to determine which side the subject is paying attention to. An online test showed that an average accuracy of about 70% could be achieved by using 3 s long data for the posterior alpha rhythm-based BCI system [23]. Overall, the gaze-independent BCI could only obtain ITRs of several bits per minute at current stage, which is much slower than that of the gaze-dependent BCI system [1, 4].

The concept of the hybrid BCI demonstrates a substantial improvement for the BCI development [24, 25]. It makes the mental control faster and more flexible through adding another channel of physiological control signals to the BCI system. Specially, the 'pure' hybrid BCI improves accuracy and universality by combining two or more different BCI systems, such as the P300-SSVEP system [26–31], SSVEP-ERD system [32–35] and P300-ERD system [36]. In particular, for the reactive BCI, the incorporation of SSVEP into other ERP paradigms would not only increase the amount of useful EEG information but also enhance typical EEG features [37], thereby facilitating the classification. Although the hybrid BCI technique has made numerous progresses, there are very few studies on applying hybrid EEG features to gaze-independent BCIs. Currently, only the combination of SSVEP and posterior alpha rhythm has been reported for controlling the gaze-independent visual BCI system [38].

This study aims to realize a fast classification of CVSA (left versus right sides) by using the hybrid EEG features including N2pc and SSVEP. The N2pc component reflects the focusing of covert attention on a peripheral location, which contains a greater negative potential in the posterior scalp when the attended item is contralateral to the recording electrode than when the attended item is ipsilateral [39]. It seems to be the earliest ERP signature on the scalp that is related to the focusing of visual attention. Therefore, through identifying the N2pc pattern, BCIs could recognize which side the subject is paying attention to. Compared with previous EEG features used in the gaze-independent BCI, the combination of N2pc and SSVEP would have several potential advantages. First, the N2pc, which often happens after 200 ms post-cue, reflects the earliest time when the visual attention becomes focused within the ventral stream [39]. So it is an important support for a fast classification. Second, when the flickering stimulus becomes focused, the SSVEP amplitude corresponding to that flickering frequency would start to increase at about 300 ms post-cue [40]. Thus the attention-modulated SSVEP would be a second indicator of the visual attention even it is weak during the N2pc period. Third, it has been demonstrated that a period of preceding SSVEPs could influence the following ERP components [30, 31, 37]. Therefore the N2pc might be enhanced under certain SSVEP modulations, which would also facilitate the subsequent classification. Based on the above analysis, this study would investigate (1) the N2pc and SSVEP characteristics of the hybrid paradigm; and (2) the performance improvement using the hybrid feature.

This paper is organized as follows. Section 2 addresses the methodology including the participants, offline experiment, feature extraction, and classification algorithms. Section 3 shows the EEG features and offline classification results. The discussion and conclusion are stated in sections 4 and 5, respectively.

2. Materials and methods

2.1. Participants

Eleven healthy volunteers (22–29 years of age; 3 females; all right handed) with normal or corrected to normal vision

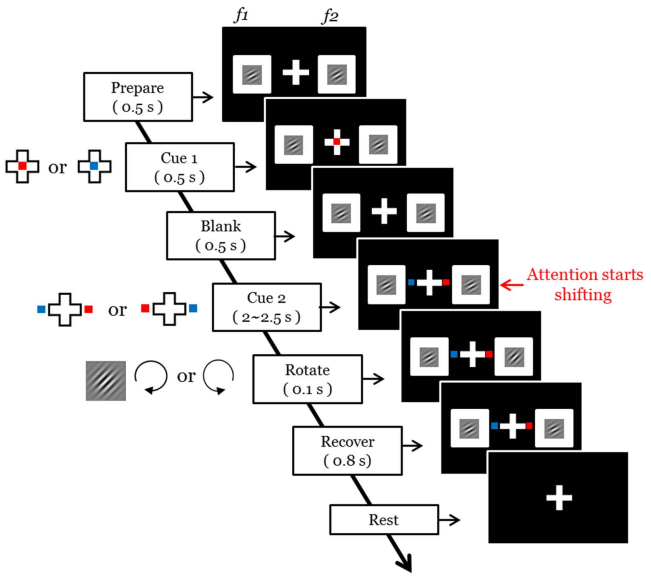

Figure 1. Temporal evolution of the stimulation of a completed trial. An example of typical stimuli is displayed on the right of the flow chart, while the key information which would be delivered during the period is shown on the left. The white squares on the left and right sides of the central cross would flicker at the frequencies of *f*1 and *f*2, respectively. There are three different frequency combinations, i.e. 10 versus 12 Hz, 12 versus 12 Hz and 0 versus 0 Hz.

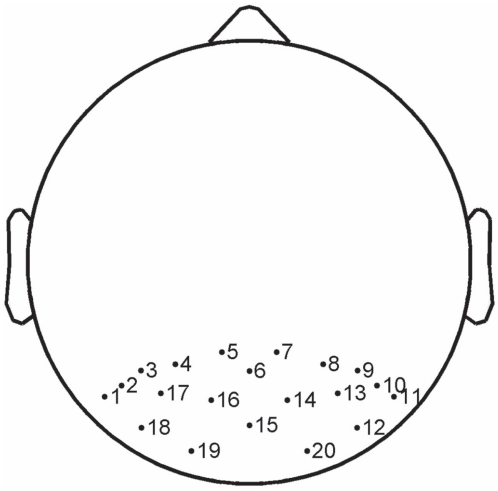

Figure 2. Active sensor locations. The numbers were regarded as their labels in this study, as the sensor locations are not according to the 10–20 international system but identified by a space position indicator. It should be noted that sensors 12, 15 and 18 correspond to PO8, POz and PO7, respectively.

participated in this study. The experimental procedures were approved by the Human Research Protections Program of the University of California San Diego. A written informed consent was obtained from all subjects after the nature and all possible consequences of the study were explained.

2.2. Experimental design and procedure

Figure 1 shows the flow chart of a completed trial. At the beginning, a preparation step would last 0.5 s. In this period, a white cross within 1° of visual angle would be displayed at the center of the screen, while two squares (11° high and 18° wide, the nearest edge to the center is 2°) on the left and right sides would flicker simultaneously at two different frequencies *f*1 and *f*2. The flicker is an alternation of white and black colors. There were three different combinations of *f*1 and *f*2 in this study. For condition '10-12', *f*1 and *f*2 were 10 Hz and 12 Hz, respectively. However, they were both 12 Hz for condition '12-12', and 0 Hz for condition '0-0' (remained white all the time). The condition '0-0' was used as the control condition for exploring the effect of SSVEP to N2pc. The selection of 10 and 12 Hz is because both of them are in the alpha band, which is deemed to be the most relevant band to the visual attention. Different combinations of these two frequencies aims to investigate the modulation on the N2pc by different background flickers. In each square, there was a Gabor patch which was a 2° spot located 7° away from the center. The dip angle of the two Gabor patches were both 45° or −45°. Then a cue of a red or blue dot (Cue 1) would be shown in the center of the cross for another 0.5 s. After that, a blank period which had the same stimulation with the preparation period would be presented for 0.5 s. Next, it displayed the second cue (Cue 2) which was either a pair of left blue and right red dots or a pair of right blue and left red dots. The dots were 1.5° away from the center. The side of the dot which shows the same color to Cue 1 was the target side. Cue 2 would last for 2 to 2.5 s indeterminably. At the end of Cue 2, the Gabor patch at the target side would rotate clockwise or anticlockwise by 15° for 0.1 s and then recover immediately for another 0.8 s. At the end, there was a rest period (2 s) during which no flickers would be presented. The paradigm which was designed by using the psychtoolbox-3 was run in the Matlab-2014 environment. During the experiment, an eye tracker (THE EYE TRIBE, 20 Hz sample rate) was used to monitor subject's eye movements. EEG was recorded by a Biosemi amplifier (2048 Hz sample rate) with 20 active sensors put on the posterior area of the scalp (see figure 2). All channels were referenced to Fz in recording. The eye tracker system and the EEG recording system were synchronized using the lab streaming layer [41].

Subjects were seated 60 cm in front of the monitor screen which was 41 × 25 cm^2 in size, having 1440 × 900 pixels and refreshing at 60 Hz. They were asked to gaze at the central cross all the time during a trial, while shift their attention covertly to the Gabor patch of the target side once Cue 2 appeared. They were asked to press a button as soon as possible when observing the rotation of the Gabor patch. The detection of Gabor patch is commonly used in the field of studying covert visual attention [42]. By analyzing the detection performance, researchers could identify those trials that the subjects successfully focus their attention to a specified location. An eligible trial required the subject to give a correct and timely response and have no eye movement during the period of Cue 2. A block consists of 24 trials, which were equally from the three conditions in a random sequence. There was a several minutes rest between two consecutive blocks. During the rest time, a quick inspection was conducted to count the number of eligible trials in the

Table 1. Candidate EEG features for classifications.

	Experimental conditions ('10-12' and '12-12')		Control condition ('0-0')	
	2–70 Hz	8–70 Hz	2–70 Hz	8–70 Hz
200–400 ms	hybrid feature (N2pc and immature SSVEP)	immature SSVEP	N2pc	/
400–600 ms,…, 1800–2000 ms	/	mature SSVEP	/	/
200–2000 ms	All features	/	/	/

past block. Two strict rejection criteria were applied in the inspection. The first criterion was that the trial would be eliminated if the eye tracker system reported an eye movement (1° from the center) or blink during the Cue 2 period. The second criterion was that the trial would not be selected if subjects did not respond in the duration of 300–800 ms after the rotation onset. Subjects were required to keep doing this task until each condition had at least 50 eligible trials for each attention side.

For the same Cue 2, subjects would either shift their attention to the left or to the right, which depended on the color of Cue 1. Therefore, the shift of attention was driven by the information previously stored in the subject's brain rather than the outside stimulus shown by Cue 2. It meant EEG features related to attention shift were endogenous in this study.

2.3. Feature extraction and classification

2.3.1. Pre-processing. In order to get a convincible result, the numbers of eligible trials were equal for all conditions, i.e. fifty for each attention side. In pre-processing, EEG signals for all 20 channels were first filtered to 0.1–100 Hz with a third order band-pass Butterworth filter, and then down-sampled at 256 Hz. For temporal waveform analysis, the EEG signals were then filtered by 3 Chebyshev Type I filters into 2–6 Hz, 9–11 Hz and 11–13 Hz for analyzing the characteristics of N2pc, 10 Hz SSVEP and 12 Hz SSVEP, respectively. The EEG samples were extracted from −500 to 2000 ms around the Cue 2 onset. For classification, the EEG signals were filtered into 2–70 Hz or 8–70 Hz by a Chebyshev Type I filter. The band of 2–70 Hz was deemed to cover the frequencies of N2pc and SSVEPs (including the harmonics), while 8–70 Hz was regarded as the frequency band of SSVEP and their harmonics in this study. The EEG samples for classification were extracted by the time windows of 200–400 ms, 400–600 ms,…, 1800–2000 ms (from 200 to 2000 ms, window length: 200 ms) and 200–2000 ms after the Cue 2 onset. As SSVEPs have a delay of about 150 ms and need almost 300 ms to reach the strongest amplitude [40], it is weak during the time segment of 200–400 ms and we referred it as the immature SSVEP in this study. Therefore, the duration of 200–400 ms contained the N2pc as well as the immature SSVEP for the experimental conditions ('10-12' and '12-12'), but it only had the N2pc for the control condition ('0-0'). As to the durations of 400–600 ms, …, 1800–2000 ms, they only contained the mature SSVEP for the experimental conditions. The duration of 200–2000 ms contained all useful EEG features including N2pc and SSVEPs. Therefore, there were five most interesting kinds of EEG features to compare in this study, which were shown in table 1.

2.3.2. N2pc and SSVEP analyzes. The N2pc is *a posterior*-contralateral negative potential with a latency of about 200–300 ms, and the CVSA modulated SSVEP is also posterior-contralateral. Thus subtracting the signal of ipsilateral attention from that of contralateral attention was the main analysis principle in this study. Specifically, for the channels on the left hemisphere, we subtracted the signal of left attention from that of right attention. Instead, for the channels on the right hemisphere, the signal of right attention were subtracted from that of left attention. After subtraction, the amplitude of N2pc was calculated as the mean amplitude within the specified time window of 180–310 ms after the Cue 2 onset, while the SSVEP amplitude was represented by its envelop which could be obtained by calculating the absolute value of the Hilbert transform of the signal. The EEG spectrum for illustration in this study was the grand average of fast Fourier transforms of single trials which contained 2 s long data after Cue 2 onset.

2.3.3. Classification algorithm. The classification of CVSA (attent to left versus attend to right) was based on canonical correlation analysis (CCA) in this study. CCA is a multichannel data processing approach which has been successfully applied to the BCI research, especially for the SSVEP-based BCI [4, 43, 44]. The standard CCA algorithm is a multivariable statistical method which aims to reveal the underlying correlation between two sets of data. It finds a pair of linear combinations for two sets to maximize the correlation between the transformed data. Consider two multidimensional random variables X, $Y \in R^{N_k \times N_s}$, where N_k is the number of channels and N_s is the length of the sample, and their linear combinations $x = X^T U_{X,Y}$ and $y = Y^T V_{X,Y}$ ($U_{X,Y}$, $V_{X,Y} \in R^{N_k \times d}$, where $d = \min$ (rank(X), rank(Y))), respectively. CCA finds the proper weight vectors, $U_{X,Y}$ and $V_{X,Y}$, to maximize the correlation between x and y. It equals to solve the following problem:

$$\mathrm{CCA}(X, Y) = \max_{U_{X,Y}, V_{X,Y}} \frac{\varepsilon[U_{X,Y}^T X Y^T V_{X,Y}]}{\sqrt{\varepsilon[U_{X,Y}^T X X^T U_{X,Y}] \cdot \varepsilon[V_{X,Y}^T Y Y^T V_{X,Y}]}}. \quad (1)$$

In the conventional method for classifying SSVEPs, X refers to the set of EEG signals and Y refers to the set of reference signals Y_f which have the same length as X. The reference

signals Y_f is set as

$$Y_f = \begin{bmatrix} \sin(2\pi \cdot fn) \\ \cos(2\pi \cdot fn) \\ \vdots \\ \sin(2\pi \cdot N_h fn) \\ \cos(2\pi \cdot N_h fn) \end{bmatrix}, \; n = \frac{1}{f_s}, \frac{2}{f_s}, \cdots, \frac{N_s}{f_s}, \tag{2}$$

where f is the fundamental frequency, f_s is the sample rate, N_h is the number of harmonics. The CCA coefficient would be large if the main oscillation frequency of X is the same with the fundamental frequency of Y_f. Therefore, the target frequency of SSVEPs could be determined by finding the maximum CCA coefficient.

In an extended approach [44], Nakanishi *et al* proposed to use the SSVEP training data $\hat{X}$ as the reference signals for frequency f, which could be obtained by averaging the training set across trials, i.e.

$$\hat{X} = \frac{1}{N}\sum_{i}^{N} X_i, \tag{3}$$

where N was the number of training samples. Moreover, three more coefficients were incorporated to classify the SSVEP. So the coefficient vector was

$$\boldsymbol{\rho} = \begin{bmatrix} \rho_1 \\ \rho_2 \\ \rho_3 \\ \rho_4 \end{bmatrix} = \begin{bmatrix} \mathrm{CCA}(X, Y_f) \\ \rho(X^T U_{X,\hat{X}}, \; \hat{X}^T U_{X,\hat{X}}) \\ \rho(X^T U_{X,Y_f}, \; \hat{X}^T U_{X,Y_f}) \\ \rho(X^T U_{\hat{X},Y_f}, \; \hat{X}^T U_{\hat{X},Y_f}) \end{bmatrix}, \tag{4}$$

where $\rho(*)$ referred to the Pearson's correlation. The final feature value was obtained by combining all coefficients, as

$$\tilde{\rho} = \sum_{i=1}^{4} \mathrm{sign}(\rho_i) \cdot \rho_i^2. \tag{5}$$

Although the CCA-based approach has been widely used in the SSVEP classification, it has never been applied to the CVSA-based BCIs. Here, we proposed a new classification strategy using the CCA algorithm, which is customized for extracting N2pc and SSVEP features during the covert attention, written as

$$\boldsymbol{\rho_k} = \begin{bmatrix} \rho_{k,1} \\ \rho_{k,2} \\ \rho_{k,3} \\ \rho_{k,4} \\ \rho_{k,5} \end{bmatrix} = \begin{bmatrix} \mathrm{CCA}(X, \hat{X}_k) \\ \rho(X^T U_{X,\hat{X}_k}, \; \hat{X}_k^T U_{X,\hat{X}_k}) \\ \rho(X^T V_{X,\hat{X}_k}, \; \hat{X}_k^T V_{X,\hat{X}_k}) \\ \rho(X^T U_{\hat{X}_k,Y_f}, \; \hat{X}_k^T U_{\hat{X}_k,Y_f}) \\ \rho(X^T U_{\hat{X}_{-k},Y_f}, \; \hat{X}_k^T U_{\hat{X}_{-k},Y_f}) \end{bmatrix}, \tag{6}$$

where k represented the attention side whose value was either -1 (left attention) or 1 (right attention), reference signal Y_f contained the flickering frequencies of both sides

$$Y_f = \begin{bmatrix} \sin(2\pi \cdot f_1 n) \\ \cos(2\pi \cdot f_1 n) \\ \sin(2\pi \cdot f_2 n) \\ \cos(2\pi \cdot f_2 n) \\ \vdots \\ \sin(2\pi \cdot N_h f_1 n) \\ \cos(2\pi \cdot N_h f_1 n) \\ \sin(2\pi \cdot N_h f_2 n) \\ \cos(2\pi \cdot N_h f_2 n) \end{bmatrix}, \; n = \frac{1}{f_s}, \frac{2}{f_s}, \cdots, \frac{N_s}{f_s}. \tag{7}$$

$\rho_{k,1}$ was the traditional CCA coefficient between X and $\hat{X}_k$, $\rho_{k,2}$, $\rho_{k,3}$, $\rho_{k,4}$ and $\rho_{k,5}$ were the Pearson's correlations between X and $\hat{X}_k$ both after spatial filtering with $U_{X,\hat{X}_k}$, $V_{X,\hat{X}_k}$, $U_{\hat{X}_k,Y_f}$ and $U_{\hat{X}_{-k},Y_f}$, respectively. More similar it was between X and $\hat{X}_k$, more larger the $\rho_{k,1}$, $\rho_{k,2}$, $\rho_{k,3}$, $\rho_{k,4}$ and $\rho_{k,5}$ would be. So the final feature value could be the sum of all squared coefficients

$$\tilde{\rho}_k = \sum_{i=1}^{5} \rho_{k,i}^2. \tag{8}$$

The predicted attention side was

$$\hat{k} = \mathrm{argmax}_k \tilde{\rho}_k. \tag{9}$$

In this study, towards a more practical BCI diagram, we performed channel selection for all three conditions, in which the best combination of two active channels and one reference channel were selected from all three-channel combinations by comparing their accuracies. In order to get a balanced comparison, Y_f matrixes were the same for all conditions, which contained both frequencies 10 and 12 Hz. Actually, as condition '12-12' had only a 12 Hz flicker and condition '0-0' had no flickers in front of subjects, the redundant frequency component in Y_f seemed useless. A further investigation found that, for these two conditions, the final accuracies were less different for different Y_f matrixes which either contained the redundant flickering frequencies or not.

3. Results

3.1. Classification performance

This study first compared the accuracies between the hybrid EEG features, i.e. the combination of N2pc and SSVEP, and the single features, i.e. the pure N2pc or SSVEP. Figure 3 shows the accuracy comparison between the hybrid feature and the single N2pc feature, and more details could be found in table 2. The EEG features for classification were extracted between 2 and 70 Hz from 200 to 400 ms for the three conditions. Therefore, conditions '10-12' and '12-12' had the combined features of N2pc and immature SSVEPs, while the '0-0' condition only contained the N2pc feature. As a result, both conditions '10-12' and '12-12' performed significantly better than condition '0-0', which could be demonstrated by the Wilcoxon signed rank test ('10-12' versus '0-0': $p = 0.004$; '12-12' versus '0-0': $p = 0.047$). Specifically, the

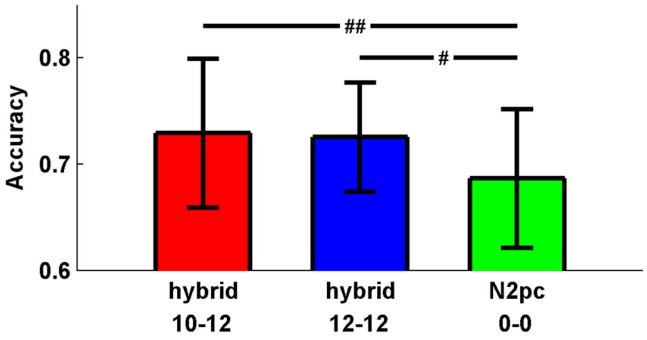

Figure 3. Accuracy comparisons between the hybrid EEG feature and the single N2pc feature. '##' means $p < 0.01$; '#' means $p < 0.05$.

average accuracy was 72.9%, 72.6% and 68.6% for conditions '10-12', '12-12' and '0-0', respectively, while the highest individual accuracy was 88%, 83% and 82%. These results indicated that the hybrid EEG features performed significantly better than the single N2pc feature.

Figure 4 shows the comparisons between the hybrid EEG feature and the single SSVEP feature. For both conditions '10-12' and '12-12', the hybrid EEG feature had a higher accuracy than the immature SSVEP and the mature SSVEP. The Wilcoxon signed rank test demonstrated that the priorities of hybrid features to immature SSVEPs were significant (for condition '10-12', $p = 0.0098$; for condition '12-12', $p = 0.012$). Specifically, the accuracy of the immature SSVEP feature was 5.27% lower than that of the hybrid EEG feature for condition '10-12', while 3.91% for condition '12-12'. For the mature SSVEP feature, the average accuracy had a loss of 2.85% and 2.51% compared with the hybrid feature for conditions '10-12' and '12-12', respectively. Therefore the hybrid EEG features also outperformed the single SSVEP feature.

Last, this study investigated the ultimate performance of the proposed paradigm. So all useful features were employed to calculate the accuracy, i.e. the feature from 200 to 2000 ms after the Cue 2 onset in the frequency band of 2–70 Hz was used. Table 2 shows the results. The average accuracies for both conditions '10-12' and '12-12' were all around 80% (79.1% versus 81.9%, $p = 0.334$). There were two subjects achieving above 90% for condition '10-12', while only one for condition '12-12'. However, the number of subjects reaching above 80% was eight for condition '12-12', which is larger than six for condition '10-12'. The peak accuracy for condition '10-12' was 93%, while that was 90% for condition '12-12'. Note that, compared with condition '0-0', the classification accuracy derived from all features was significantly improved for both conditions '10-12' and '12-12' ('10-12' versus '0-0': 79.1% versus 66.2%, $p < 0.001$; '12-12' versus '0-0': 81.9% versus 66.2%, $p < 0.001$).

3.2. N2pc analysis

To show how the ongoing SSVEP modulates the N2pc, this study compared the N2pc differences among different conditions. Figure 5 shows the temporal and spatial features of the N2pc for all conditions. The left N2pc was obtained by subtracting the EEG of left attention from that of right attention, while it was in reverse for the right N2pc. From an overall view of the N2pc distribution displayed in the middle subgraphs, conditions '12-12' and '0-0' had a similar topography, which was very different from that of condition '10-12'. Generally, the '12-12' and '0-0' conditions showed an obviously larger and wider N2pc for the left hemisphere than the right hemisphere, but the right N2pc seemed to be larger and wider than the left one for condition '10-12'. A further analysis on specified locations showed that for the left N2pc, the amplitudes of the three conditions were similar, but for the right one, condition '10-12' showed significantly larger amplitude than the others, which could be demonstrated by the Wilcoxon signed rank test ('10-12' versus '12-12': $p = 0.042$; '10-12' versus '0-0': $p = 0.005$). In particular, the left N2pc amplitude was $0.32 \pm 0.26\,\mu$V, $0.52 \pm 0.48\,\mu$V and $0.46 \pm 0.44\,\mu$V for conditions '10-12', '12-12' and '0-0', respectively, while the right N2pc amplitude was $0.58 \pm 0.33\,\mu$V, $0.18 \pm 0.42\,\mu$V and $0.24 \pm 0.20\,\mu$V.

3.3. SSVEP analysis

The SSVEP response is another important character in this study. Figure 6 shows the spectrum differences of SSVEPs between attending left and right. For condition '10-12', attending left induced a significantly larger 10 Hz SSVEP than attending right (left versus right: 0.609 μV versus 0.573 μV, $p = 0.042$), revealed by the Wilcoxon signed rank test. However, on the contrary, the amplitude of 12 Hz was significantly larger for attending right than attending left (left versus right: 0.622 μV versus 0.656 μV, $p = 0.032$). It was in accordance with the experimental design that the 10 Hz flicker was in the left visual field while the 12 Hz in the right visual field in this condition. For condition '12-12', the 12 Hz amplitude of attending left was 0.511 μV, which was slightly less than 0.542 μV of attending right. However, there was no significant difference between them ($p = 0.278$), which could be easily explained by that there was a same 12 Hz flickering square in both visual fields. For condition '0-0', no SSVEP peaks could be found in the spectrum, as no flickers were displayed in front of subjects in this condition.

For a better understanding of the SSVEP characteristic in this study, figure 7 displays the amplitudes of 10 Hz EEG oscillations for different conditions after subtraction. It is clearly shown that the three lines in the left hemisphere almost fluctuated in the same level from −500 to 2000 ms after Cue 2 onset. A further analysis on the N2pc duration did not find any significant differences among the three conditions. It indicated that the experimental conditions had almost the same amount of 10 Hz EEG oscillations with the control condition, which was in accord with the fact that no 10 Hz flicker appeared in the right visual field for the three conditions. For the right hemisphere, the lines of conditions '12-12' and '0-0' stayed together and kept stable throughout the time. As to condition '10-12', it first kept at a low level just as the others, then started to increase for a period of about 500 ms

Table 2. Accuracies obtained by using 0.2–0.4 s and 0.2–2 s data, respectively.

Subject		1	2	3	4	5	6	7	8	9	10	11	Ave.
'10-12'	0.2–0.4 s	0.88	0.72	0.75	0.74	0.63	0.71	0.65	0.81	0.74	0.68	0.71	0.729
	0.2–2 s	0.93	0.80	0.91	0.85	0.66	0.77	0.63	0.75	0.84	0.80	0.76	0.791
'12-12'	0.2–0.4 s	0.83	0.68	0.72	0.76	0.74	0.71	0.63	0.76	0.74	0.72	0.69	0.726
	0.2–2 s	0.88	0.73	0.88	0.87	0.80	0.90	0.66	0.83	0.89	0.76	0.80	0.819
'0-0'	0.2–0.4 s	0.82	0.73	0.68	0.64	0.61	0.71	0.62	0.76	0.67	0.62	0.69	0.686
	0.2–2 s	0.77	0.65	0.67	0.58	0.64	0.65	0.58	0.71	0.69	0.70	0.64	0.662

and then reached to an obviously higher level around 1600 ms after the Cue 2 onset. It conformed to the experimental design that only condition '10-12' had a flicker of 10 Hz on the left visual field. There was no significant difference of SSVEPs among the three conditions during the N2pc period.

Figure 8 displays the amplitudes of 12 Hz EEG oscillations of different conditions after subtraction. For the left hemisphere, the three lines were not separated until about 400 ms after the Cue 2 onset. Conditions '10-12' and '12-12' had an increasing trend after that time, while condition '0-0' remained at the same level, which conformed to the fact that the experimental conditions had a 12 Hz flicker in the right visual field but the control condition did not have. The growth rate was obviously larger for condition '12-12' than condition '10-12'. After a growth lasting 400 ms, the two conditions stepped into a new stable period from about 800 ms to the end. No significant difference could be found in the N2pc period for the three conditions. For the right hemisphere, condition '12-12' showed an evident ascending trend after 400 ms, while the changes of the other lines were not obvious. The line of condition '12-12' was evidently higher than the others from 800 ms to the end, which was in accord with that only the '12-12' condition would produce a 12 Hz SSVEP on the right hemisphere. A further analysis on the N2pc period did not find any significant difference for 12 Hz amplitudes among the three conditions.

4. Discussion

4.1. Comparison with previous studies

To verify the advancement of the proposed paradigm, the results of this study were compared with that of previous works on the gaze-independent BCI, shown in table 3. For convenience, the estimated theoretical ITR was calculated from the average accuracy in this table and the time cost for each selection did not include the break between selections, so it might be different from other references. It could be found that the P300, SSVEP and alpha rhythm were the most popular signals used in the gaze-independent BCIs. Generally speaking, the consuming time for sending a command was longer than 2 s in the past work. Specifically, by using the P300, the classes of commands could be as many as 30 or more, and the accuracy could be above 90%. However, it costs tens of seconds for each output, which greatly affects the ITR (only around 10 bit min^{-1}). It should be noted Yin *et al* developed a high-efficiency gaze-independent BCI by using non-visual bimodal P300, which could achieve about 15 bit min^{-1}. For the studies using the SSVEP or/and alpha rhythm signals, the operation time for each output could be reduced to around 4 s. However, there were only 2 or 4 classes and the average accuracy was near 70%. Therefore, the estimated ITR was also only several bits min^{-1}. Overall, the speed and ITR of conventional gaze-independent BCIs were very low, which could not meet the actual needs. This study proposed a new paradigm which could have a fast classification within 400 ms and an acceptable accuracy around 72.9%. As a result, the estimated theoretical ITR could be as high as 23.56 bits min^{-1} which was greatly higher than that reported in previous studies. Note that, the practical ITR in real use is generally lower due to the inclusion of data analysis, feedback presentation, and determination of a target.

4.2. No exogenous information used in the classification

The main reason for infeasibility of gaze-dependent BCIs for severe ALS patients is that the exogenous ERP components which play an important role in classifications become significantly smaller than those can be evoked in the healthy people. Therefore, the conventional paradigms and classification methods are impracticable when being applied to clinical tests. As the EEG features modulated by the exogenous stimulation were never useful for an gaze-independent BCI, researchers started focusing their attention on the endogenous EEG features, such as the P300 potential, posterior alpha rhythm and the attention-modulated SSVEP. In previous offline studies, targets that were located in different places were often be indicated by arrows with different directions [22, 23]. Although the physical differences between the visual cues might not produce an obvious EEG difference, it risked evoking ERPs specific to the direction of the cue. In this study, no exogenous information related to the attention direction was used in the classification. Subjects must shift their attention based on the target color which was previously stored in their minds. For example, when the Cue 2 appears as a pair of left red and right blue dots, subjects have to shift their attention to the left if looking for the red dot, but to the right if blue. The EEG differences between the left and right attentions were completely induced by the endogenous factor. Therefore, the proposed paradigm is

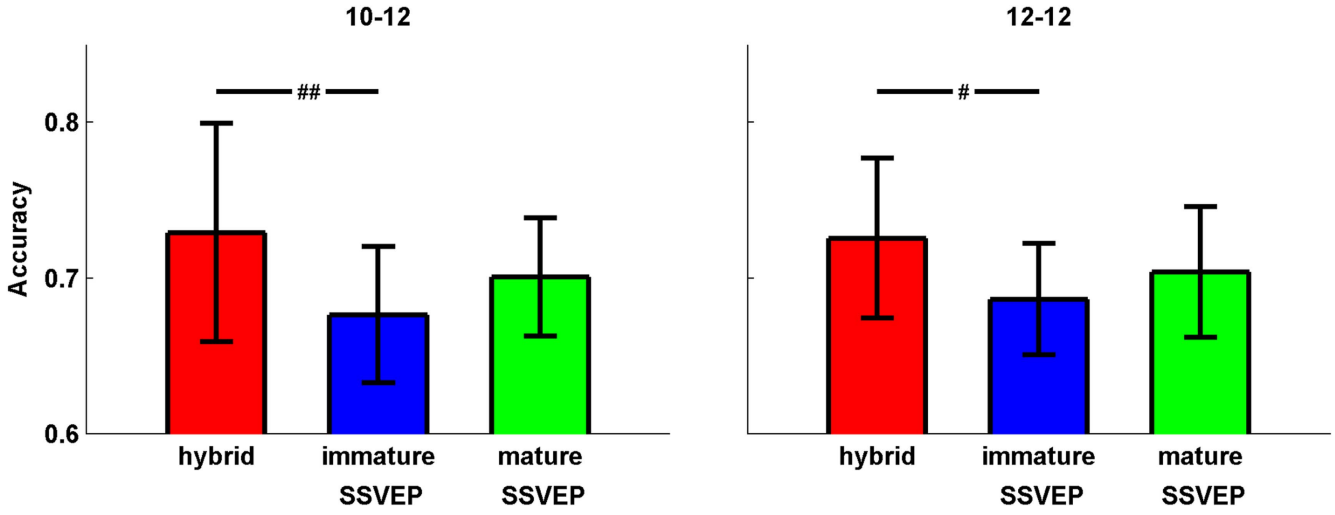

Figure 4. Accuracy comparisons between the hybrid EEG features and the single SSVEP feature. '##' means $p < 0.01$; '#' means $p < 0.05$.

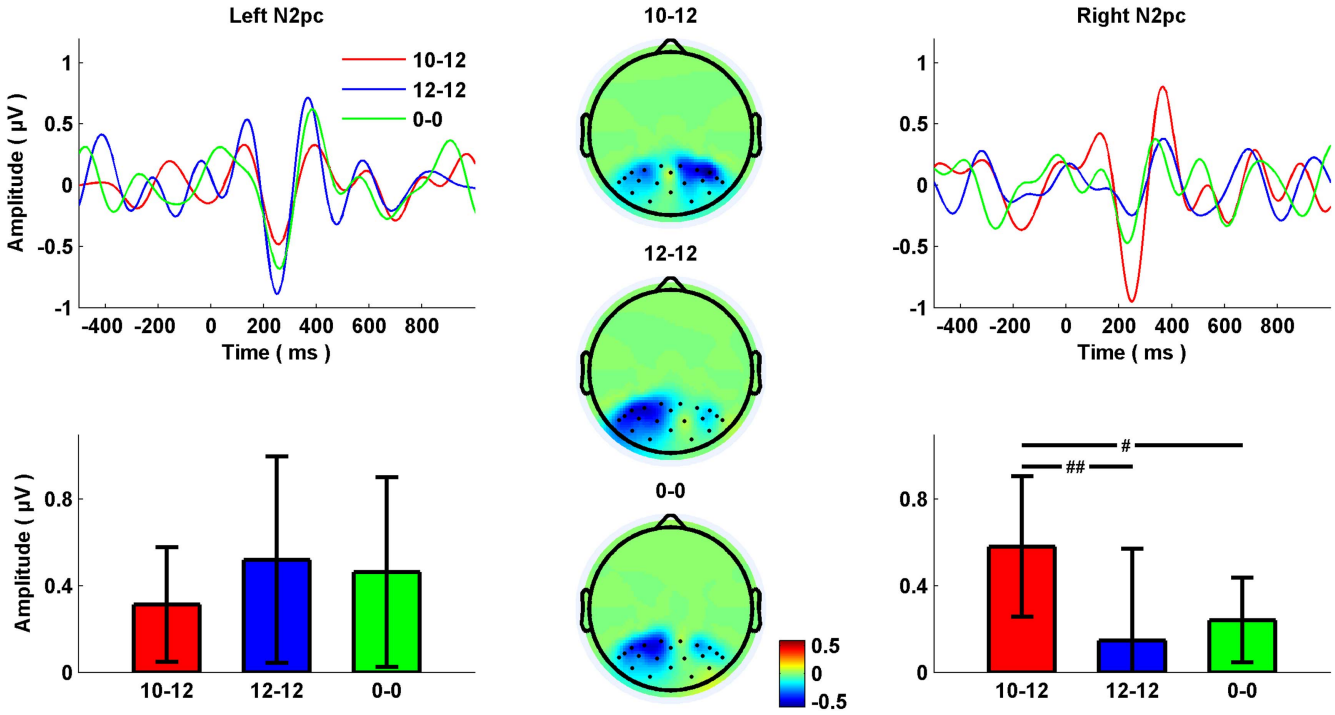

Figure 5. Grand average N2pc potential across subjects. The left most column shows the N2pc temporal waves (top) and amplitudes (bottom) for the left hemisphere, while the right most one is for the right hemisphere. The left N2pc was calculated from the average of channels 3 and 4, while the right one was the average of channels 8 and 9. The selections of channel 3, 4, 8 and 9 are because the N2pc potentials are most significant in these locations. The middle column displays the N2pc topographies of the three conditions. '##' means $p < 0.01$; '#' means $p < 0.05$. 0 ms is the onset of Cue 2.

effective for developing an online gaze-independent BCI system, in which the attention side is self-chosen by the user.

4.3. Hybrid feature for gaze-independent BCIs

Most studies on gaze-independent BCIs rely on only one type of EEG feature. Normally, the SSVEP, P300 and alpha rhythm are the three most popular features for this topic. However, as the brain response to outside stimulation become significantly weaker for the covert attention than the overt one, the performances of SSVEP and P300 would deteriorate correspondingly. Although the distribution of posterior alpha rhythm could be an indicator of the brain state, it seems not as effective as the other two features. The hybrid BCI was proposed to combine two or more physiological signals (at least one is the EEG) to control the system. Specifically, the pure hybrid BCI only uses variety of EEG features as the control signal. It is quite popular for the gaze-dependent BCI, and shows an advantage over the conventional system. However, few studies have developed a hybrid gaze-

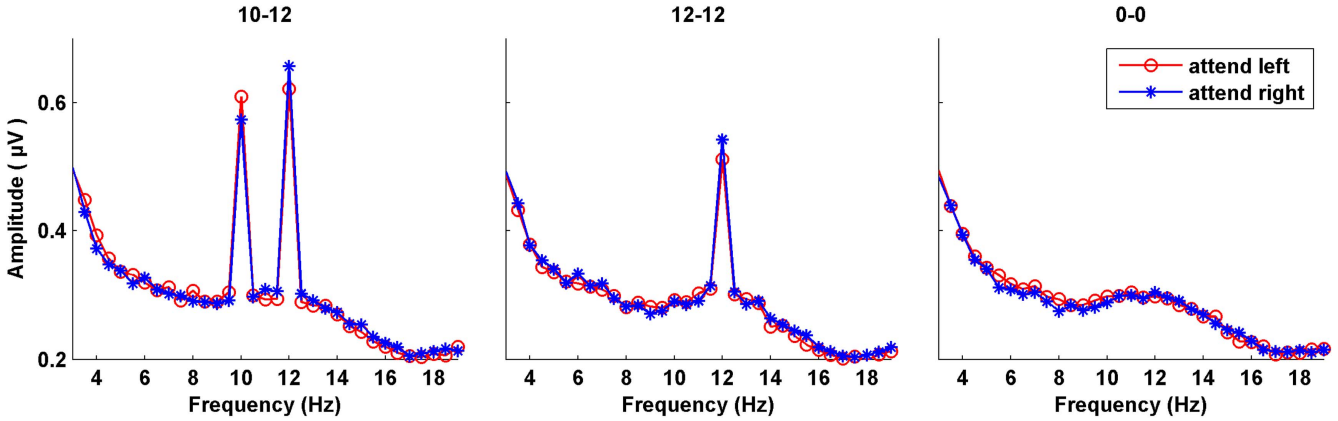

Figure 6. Grand average EEG spectra across subjects for the three different conditions. The data are collapsed across channels 1, 2, 10 and 11. We did not choose the same locations in the N2pc analysis, because there were no significant differences between attending left and right in those areas. The reason might be the stimulation inducing SSVEPs are located at more lateral area than that inducing N2pc in this study. According to visual pathway in the brain, the more lateral image maps to the more lateral visual cortex, so the appropriate area for SSVEP analyzes may be located outer than that for N2pc.

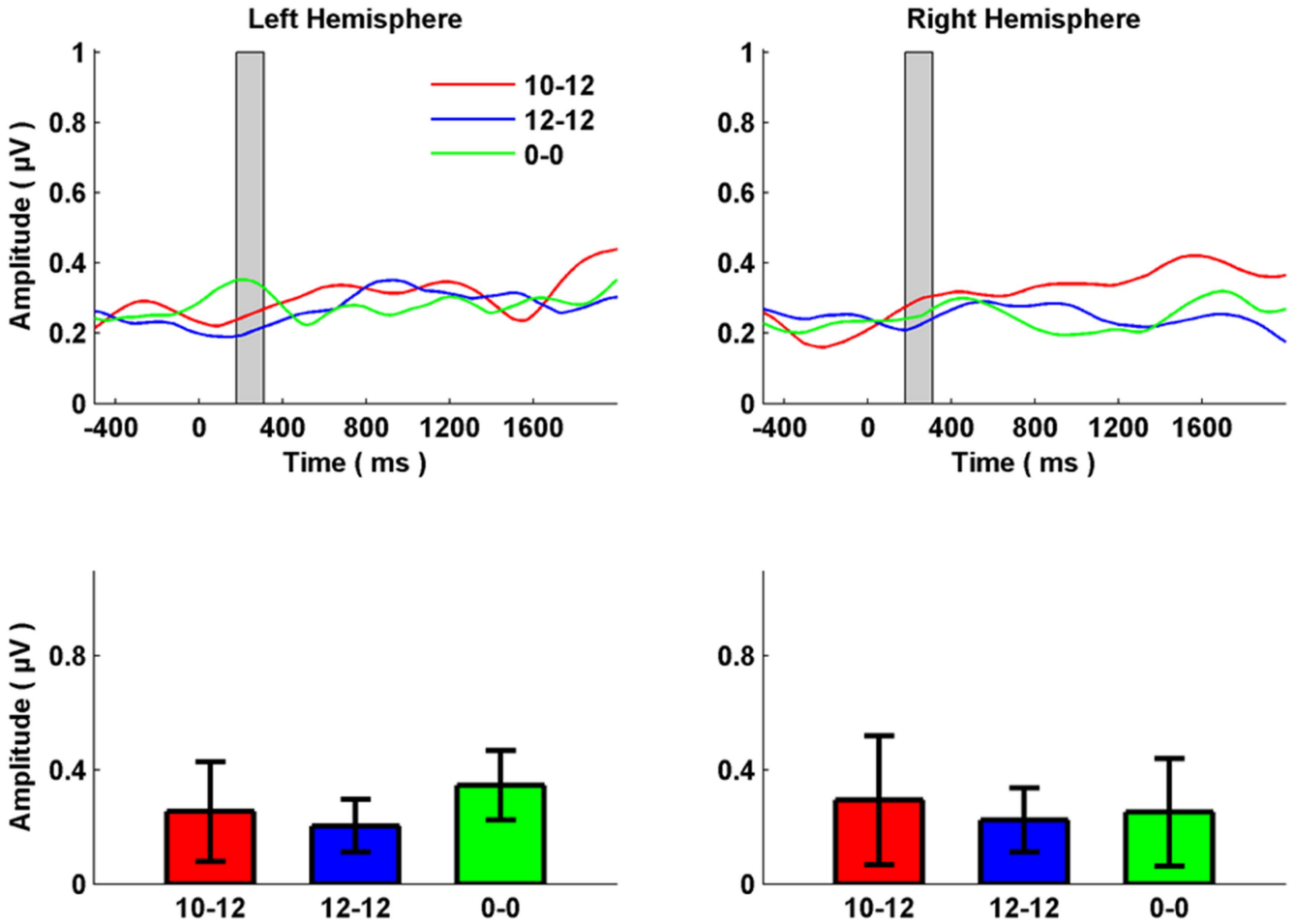

Figure 7. Grand average amplitudes of 10 Hz EEG oscillations across subjects. The left subgraphs show the amplitudes of EEG oscillations recorded from the average of channels 1 and 2 which are in the left hemisphere, while the right ones are the average of channels 10 and 11 which are in the right hemisphere. The bottom histograms show the average amplitudes during the N2pc period. 0 ms is the onset of Cue 2.

independent BCI. Kelly *et al* first proposed to use the combined features of posterior alpha rhythm and SSVEP for classifying the CVSA [38]. It demonstrated that the hybrid feature was more effective than the single one in tracking the visual spatial attention. However, it required a long time (~3.39 s) to get an acceptable accuracy. This study designed a new gaze-independent paradigm to evoke both the N2pc and SSVEP features during the covert visual attention. N2pc

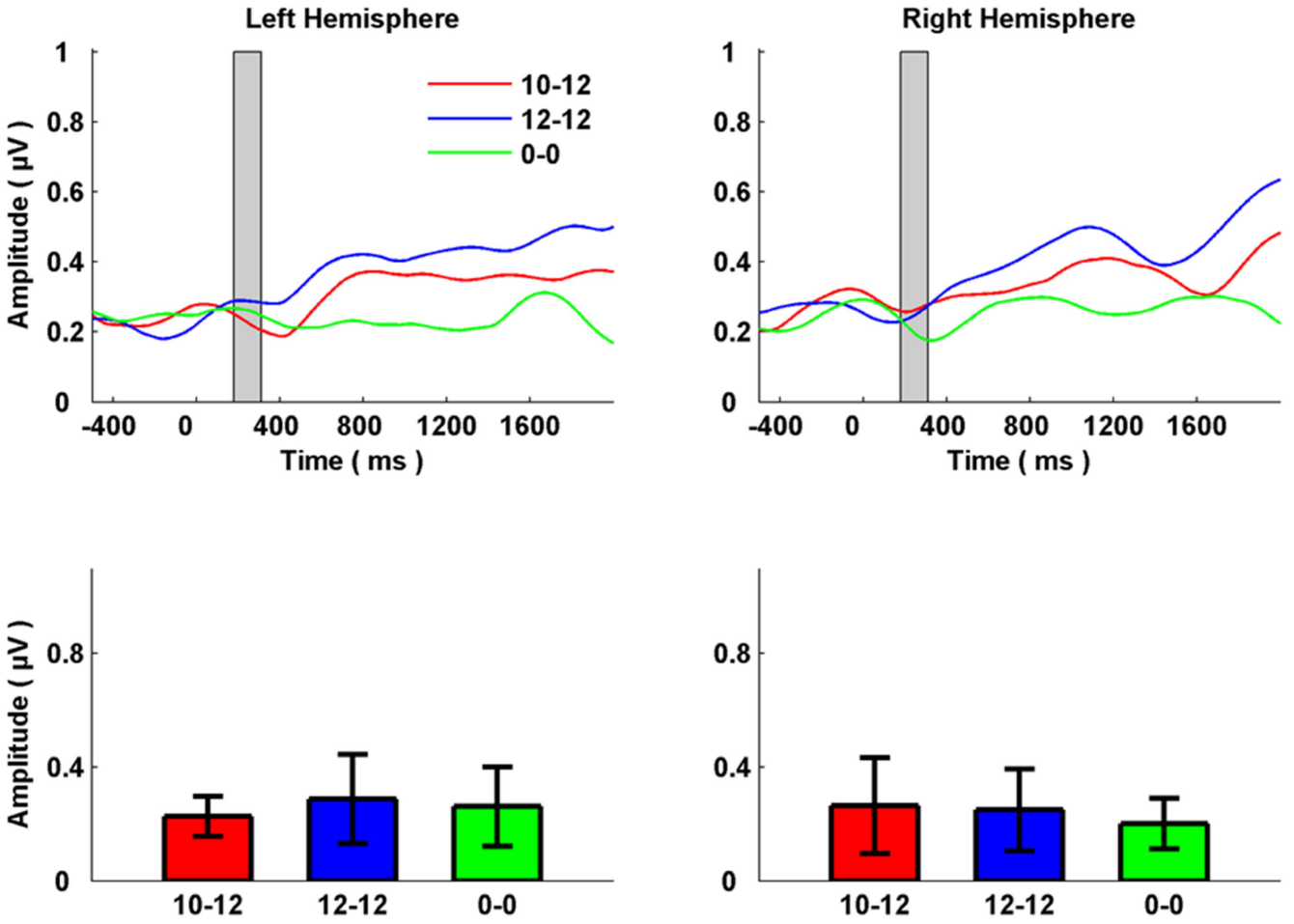

Figure 8. Grand average amplitudes of 12 Hz EEG oscillations across subjects. The left subgraphs show the amplitudes of EEG oscillations recorded from the average of channels 1 and 2 which are in the left hemisphere, while the right ones are the average of channels 10 and 11 which are in the right hemisphere. The bottom histograms show the average amplitudes during the N2pc period. 0 ms is the onset of Cue 2.

appears on the opposite side to the visual stimuli of interest to the subject. So it is related to the process of selective attention. Its feasibility in constructing BCI systems has been demonstrated by previous studies [47, 48]. This study first combined it with the covert attention-modulated SSVEP to realize a gaze-independent BCI system. The results show that, compared with the single N2pc feature and the immature SSVEP within 400 ms after the shift of attention, the combination of them could achieve a significantly higher accuracy with an average of 72.9% and a peak of 88%. When 2 s long data were applied, the hybrid EEG feature could obtain an average accuracy of about 80%. As the conventional approach often needs more than 3 s to estimate the covert attention state, our proposed method is indeed promising for a fast classification of CVSA.

4.4. SSVEP effects on N2pc

Another interesting phenomenon which should be discussed is the SSVEP effects on the N2pc. It could be obviously found from figure 5 that the right N2pc of condition '10-12' was significantly larger than those of conditions '0-0' and '12-12'. These findings suggest that the N2pc attributes could be influenced by the background SSVEPs. It is quite a useful message for exploring the ERP mechanism which has a long-time debate between the evoked model and the oscillation model. The evoked model holds the view that ERPs are a fixed-polarity and a fixed-latency neural response which is superimposed onto the background EEG, while the oscillation model argues that ERPs are generated by the partial phase resetting of ongoing EEG oscillations [49]. As the ERP is so small that it is often submerged under the background EEG, a large number of trials are required to be averaged for a clear ERP waveform. However, one problem in the traditional approach to the average ERP is that the zero-mean baseline which is deprived of the dynamic information could not provide a clear ERP initial state, thereby seeming less useful for evaluating the ERP dynamics. Xu *et al* proposed a new method of using the steady-state baseline (i.e. a period of SSVEP) to investigate the evolution process of visual evoked potentials, in which the ERP initial state could be modulated into a specified oscillation [37]. It revealed a 'three-period-transition' for the generation of visual N1 and found a strong evidence to balance the two contradictory models on N1. However, the steady-state baseline has yet been applied to the N2pc mechanism. As the N2pc is an endogenous potential,

Table 3. List of studies on gaze-independent BCIs.

Reference	Subjects	Signal	Feature	Classification method	Classes	Time cost (s)	Average accuracy (%)	Estimated ITR (bit min^{-1})
Kelly *et al* 2005 [9]	11 (healthy)	SSVEP	Spectral power	Threshold	2	4–12	~61.6	<1
Kelly *et al* 2005 [38]	10 (healthy)	SSVEP + alpha rhythm	Spectral power	Linear discriminant analysis(LDA)	2	3.39	79.5	4.75
Gerven *et al* 2009 [20]	15 (healthy)	Alpha rhythm	Spectral power	Support vector machine	4	2.5	41	2.12
Zhang *et al* 2010 [11]	18 (healthy)	SSVEP	CCA coefficients	LDA	2	4	72.6	2.29
Treder *et al* 2011 [15]	13 (healthy)	P300	Temporal wave	LDA	36	25	97.1	11.60
Treder *et al* 2011 [21]	8 (healthy)	Alpha rhythm	Spectral power	Logistic regression	2	2	74.6	5.47
Liu *et al* 2011 [14]	8 (healthy)	P300	Temporal wave	Stepwise LDA	36	20.3	84.1	11.00
Schaeff *et al* 2012 [16]	16 (healthy)	Motion VEP	Temporal wave	LDA	30	32.65	96.2	8.25
Aloise *et al* 2012 [17]	10 (healthy)	P300	Temporal wave	Stepwise LDA	36	24.55	77.8	7.99
Andersson *et al* 2012 [45]	9 (healthy)	BLOD signal	Image volume	Threshold	4	6.48	79.4	8.7
Tonin *et al* 2013 [23]	8 (healthy)	Alpha rhythm	Spectro-temporal pattern	Quadratic discriminant analysis	2	3	70.6	2.37
Acqualagna *et al* 2013 [18]	12 (healthy)	P300	Temporal wave	Shrinkage LDA	30	28.72	93.6	8.88
Marchetti *et al* 2013 [19]	10 (ALS)	P300	Temporal wave	SVM	4	6	71.39	6.83
Lesenfants *et al* 2014 [12]	24 (healthy)	SSVEP	Combination of spectral power, CCA coefficients and lock-in feature	LDA or SVM	2	7	~80	2.38
	6 (ALS)						~61	<1
Yin *et al* 2016 [46]	12(healthy)	Bimodal P300	Temporal wave	Bayesian LDA	4	5.27	88.67	14.94
This study	11(healthy)	SSVEP + N2pc	CCA coefficients	Threshold	2	0.4	72.9	23.56
						2	81.9	9.53

which is different from the N1 that is exogenous, the feasibility of the SSVEP-based steady-state baseline remains unknown. This study proposed a new paradigm which could induce a period of SSVEP before the N2pc. It found that the N2pc attribute is relevant to the baseline, so the steady-state baseline also works for the N2pc potential even it is endogenous. Compared with condition '12-12', condition '10-12' had a stronger 10 Hz oscillation on the right hemisphere. It could be a possible reason for the larger right N2pc in condition '10-12', as the 10 Hz might be a special frequency to the N2pc. But another possible explanation to the larger N2pc might be the asymmetric stimulation, i.e. the left 10 and right 12 Hz flickers. Therefore, it remains an open question what factors would have an influence on the N2pc attribute.

5. Conclusion

This study first proposed to use the combination of the N2pc and the attention-modulated SSVEP features to track the CVSA. A new paradigm was designed to link users' endogenous activities with their attention shifts, and a new classification strategy based on CCA was developed to decode the CVSA side. Experimental results showed that the N2pc amplitude would be augmented by certain background SSVEPs. The offline classification analysis indicated that the left vs. right covert attention could be effectively classified by using the hybrid EEG features within a short time window, which demonstrated that the proposed method could be a promising approach for an efficient gaze-independent BCI system.

Acknowledgments

This paper was supported by National Natural Science Foundation of China (Grant No. 91520205, 81571762 and 31500865), Tianjin Key Technology R&D Program (No. 15ZCZDSY00930), Natural Science Foundation of Tianjin (No.15JCYBJC29600), and the Recruitment Program for Young Professionals.

References

[1] Gao S, Wang Y, Gao X and Hong B 2014 Visual and auditory brain–computer interfaces *IEEE Trans. Biomed. Eng.* **61** 1436–47

[2] Nicolas-Alonso L F and Gomez-Gil J 2012 Brain computer interfaces, a review *Sensors* **12** 1211–79

[3] Jin J, Allison B Z, Zhang Y, Wang X and Cichocki A 2014 An ERP-based BCI using an oddball paradigm with different faces and reduced errors in critical functions *Int. J. Neural Syst.* **24** 1450027

[4] Chen X, Wang Y, Nakanishi M, Gao X, Jung T P and Gao S 2015 High-speed spelling with a noninvasive brain–computer interface *Proc. Natl Acad. Sci. USA* **112** E6058–67

[5] Yao L, Meng J, Sheng X, Zhang D and Zhu X 2015 A novel calibration and task guidance framework for motor imagery BCI via a tendon vibration induced sensation with kinesthesia illusion *J. Neural Eng.* **12** 016005

[6] Sellers E W, Vaughan T M and Wolpaw J R 2010 A brain–computer interface for long-term independent home use *Amyotroph. Lateral Scler.* **11** 449–55

[7] Nijboer F *et al* 2008 A P300-based brain–computer interface for people with amyotrophic lateral sclerosis *Clin. Neurophysiol.* **119** 1909–16

[8] Brunner P, Joshi S, Briskin S, Wolpaw J R, Bischof H and Schalk G 2010 Does the 'P300' speller depend on eye gaze? *J. Neural Eng.* **7** 056013

[9] Kelly S P, Lalor E C, Finucane C, McDarby G and Reilly R B 2005 Visual spatial attention control in an independent brain–computer interface *IEEE Trans. Biomed. Eng.* **52** 1588–96

[10] Allison B Z, McFarland D J, Schalk G, Zheng S D, Jackson M M and Wolpaw J R 2008 Towards an independent brain–computer interface using steady state visual evoked potentials *Clin. Neurophysiol.* **119** 399–408

[11] Zhang D, Maye A, Gao X, Hong B, Engel A K and Gao S 2010 An independent brain–computer interface using covert non-spatial visual selective attention *J. Neural Eng.* **7** 016010

[12] Lesenfants D *et al* 2014 An independent SSVEP-based brain–computer interface in locked-in syndrome *J. Neural Eng.* **11** 035002

[13] Treder M S and Blankertz B 2010 (C)overt attention and visual speller design in an ERP-based brain–computer interface *Behav. Brain Funct.* **6** 28

[14] Liu Y, Zhou Z and Hu D 2011 Gaze independent brain–computer speller with covert visual search tasks *Clin. Neurophysiol.* **122** 1127–36

[15] Treder M S, Schmidt N M and Blankertz B 2011 Gaze-independent brain–computer interfaces based on covert attention and feature attention *J. Neural Eng.* **8** 066003

[16] Schaeff S, Treder M S, Venthur B and Blankertz B 2012 Exploring motion VEPs for gaze-independent communication *J. Neural Eng.* **9** 045006

[17] Aloise F, Aricò P, Schettini F, Riccio A, Salinari S, Mattia D, Babiloni F and Cincotti F 2012 A covert attention P300-based brain–computer interface: geospell *Ergonomics* **55** 538–51

[18] Acqualagna L and Blankertz B 2013 Gaze-independent BCI-spelling using rapid serial visual presentation (RSVP) *Clin. Neurophysiol.* **124** 901–8

[19] Marchetti M, Piccione F, Silvoni S, Gamberini L and Priftis K 2013 Covert visuospatial attention orienting in a brain–computer interface for amyotrophic lateral sclerosis patients *Neurorehabil Neural Repair.* **27** 430–8

[20] Van Gerven M and Jensen O 2009 Attention modulations of posterior alpha as a control signal for two-dimensional brain–computer interfaces *J. Neurosci. Methods* **179** 78–84

[21] Treder M S, Bahramisharif A, Schmidt N M, van Gerven M A and Blankertz B 2011 Brain–computer interfacing using modulations of alpha activity induced by covert shifts of attention *J. Neuroeng. Rehabil.* **8** 24

[22] Tonin L, Leeb R and Del R Millán J 2012 Time-dependent approach for single trial classification of covert visuospatial attention *J. Neural Eng.* **9** 045011

[23] Tonin L, Leeb R, Sobolewski A and del R Millán J 2013 An online EEG BCI based on covert visuospatial attention in absence of exogenous stimulation *J. Neural Eng.* **10** 056007

[24] Müller-Putz G R *et al* 2011 Tools for brain–computer interaction: a general concept for a hybrid BCI *Front. Neuroinform.* **5** 30

[25] Pfurtscheller G, Allison B Z, Brunner C, Bauernfeind G, Solis-Escalante T, Scherer R, Zander T O, Mueller-Putz G, Neuper C and Birbaumer N 2010 The hybrid BCI *Front. Neurosci.* **4** 30

[26] Panicker R C, Puthusserypady S and Sun Y 2011 An asynchronous P300 BCI with SSVEP-based control state detection *IEEE Trans. Biomed. Eng.* **58** 1781–8
[27] Yin E, Zhou Z, Jiang J, Chen F, Liu Y and Hu D 2013 A novel hybrid BCI speller based on the incorporation of SSVEP into the P300 paradigm *J. Neural Eng.* **10** 026012
[28] Yin E, Zhou Z, Jiang J, Chen F, Liu Y and Hu D 2014 A speedy hybrid BCI spelling approach combining P300 and SSVEP *IEEE Trans. Biomed. Eng.* **61** 473–83
[29] Yin E, Zeyl T, Saab R, Chau T, Hu D and Zhou Z 2015 A hybrid brain–computer interface based on the fusion of P300 and SSVEP scores *IEEE Trans. Neural Syst. Rehabil. Eng.* **23** 693–701
[30] Xu M, Qi H, Wan B, Yin T, Liu Z and Ming D 2013 A hybrid BCI speller paradigm combining P300 potential and the SSVEP blocking feature *J. Neural Eng.* **10** 026001
[31] Xu M, Chen L, Zhang L, Qi H, Ma L, Tang J, Wan B and Ming D 2014 A visual parallel-BCI speller based on the time–frequency coding strategy *J. Neural Eng.* **11** 026014
[32] Allison B Z, Brunner C, Kaiser V, Müller-Putz G R, Neuper C and Pfurtscheller G 2010 Toward a hybrid brain–computer interface based on imagined movement and visual attention *J. Neural Eng.* **7** 26007
[33] Brunner C, Allison B Z, Krusienski D J, Kaiser V, Müller-Putz G R, Pfurtscheller G and Neuper C 2010 Improved signal processing approaches in an offline simulation of a hybrid brain–computer interface *J. Neurosci. Methods* **188** 165–73
[34] Pfurtscheller G, Solis-Escalante T, Ortner R, Linortner P and Müller-Putz G R 2010 Self-paced operation of an SSVEP-based orthosis with and without an imagery-based 'brain switch:' a feasibility study towards a hybrid BCI *IEEE Trans. Neural Syst. Rehabil. Eng.* **18** 409–14
[35] Horki P, Solis-Escalante T, Neuper C and Müller-Putz G 2011 Combined motor imagery and SSVEP based BCI control of a 2 DoF artificial upper limb *Med. Biol. Eng. Comput.* **49** 567–77
[36] Long J, Li Y, Yu T and Gu Z 2012 Target selection with hybrid feature for BCI-Based 2D cursor control *IEEE Trans. Biomed. Eng.* **59** 132–40
[37] Xu M *et al* 2016 Use of a steady-state baseline to address evoked versus oscillation models of visual evoked potential origin *Neuroimage* **134** 204–12
[38] Kelly S P, Lalor E C, Reilly R B and Foxe J J 2005 Visual spatial attention tracking using high-density SSVEP data for independent brain–computer communication *IEEE Trans. Neural Syst. Rehabil. Eng.* **13** 172–8
[39] Luck S J, Kappenman E S, Luck S J and Kappenman E S 2012 ERP components and selective attention *The Oxford Handbook of Event-Related Potential Components* (Oxford: Oxford University Press) pp 295–328
[40] Müller M M, Teder-Sälejärvi W and Hillyard S A 1998 The time course of cortical facilitation during cued shifts of spatial attention *Nat. Neurosci.* **1** 631–4
[41] Kothe C A and Makeig S 2013 BCILAB: a platform for brain–computer interface development *J. Neural Eng.* **10** 056014
[42] Carrasco M, Ling S and Read S 2004 Attention alters appearance *Nat. Neurosci.* **7** 308–13
[43] Bin G, Gao X, Yan Z, Hong B and Gao S 2007 An online multi-channel SSVEP-based brain–computer interface using a canonical correlation analysis method *J. Neural Eng.* **6** 046002
[44] Nakanishi M, Wang Y, Wang Y T, Mitsukura Y and Jung T P 2014 A high-speed brain speller using steady-state visual evoked potentials *Int. J. Neural Syst.* **24** 1450019
[45] Andersson P, Ramsey N F, Raemaekers M, Viergever M A and Pluim J P 2012 Real-time decoding of the direction of covert visuospatial attention *J. Neural Eng.* **9** 045004
[46] Yin E, Zeyl T, Saab R, Hu D, Zhou Z and Chau T 2016 An auditory-tactile visual saccade-independent P300 brain–computer interface *Int. J. Neural Syst.* **26** 1650001
[47] Awni H, Norton J J, Umunna S, Federmeier K D and Bretl T 2013 Towards a brain computer interface based on the N2pc event-related potential *6th Int. IEEE/EMBS Conf. on Neural Engineering (NER), 2013 (San Diego, CA, 6–8 November 2013)* pp 1021–4
[48] Matran-Fernandez A and Poli R 2014 Collaborative brain–computer interfaces for target localisation in rapid serial visual presentation *6th Computer Science and Electronic Engineering Conf. (Colchester, 25–26 September 2014)* pp 127–32
[49] Sauseng P, Klimesch W, Gruber W R, Hanslmayr S, Freunberger R and Doppelmayr M 2007 Are event-related potential components generated by phase resetting of brain oscillations? A critical discussion *Neuroscience* **146** 1435–44